Inorg. Chem. **2002**, *41*, 874–883

Photochemistry and Photophysics of Cr(III) Macrocyclic Complexes

G. Irwin,[†] A. D. Kirk,*[,†] I. Mackay,[‡] and J. Nera[†]

Department of Chemistry, University of Victoria, P.O. Box 3065, Victoria, British Columbia, Canada V8W 3V6, and Chemistry Department, Southern Alberta Institute of Technology, 1301 16th Avenue Northwest, Calgary, Alberta, Canada T2M 0L4

Received March 1, 2001

The phosphorescence and photochemical behavior of the macrocyclic complexes (1,4,7,10,13,16-hexaazacyclooctadecane)chromium(III) ($Cr([18]\text{-}aneN_6)^{3+}$; **1**) and (4,4′,4″-ethylidynetris(3-azabutan-1-amine)) chromium(III) ($Cr(sen)^{3+}$; **2**) have been compared to each other and to the complex $Cr(en)_3^{3+}$. For both macrocyclic complexes, phosphorescence from room temperature aqueous solutions is too weak to be observed, contrasting with $Cr(en)_3^{3+}$, though both had somewhat longer 77 K lifetimes than $Cr(en)_3^{3+}$. Phosphorescence lifetimes for these macrocyclics decreased with increasing temperature much faster than for $Cr(en)_3^{3+}$ and a conventional extrapolation based on a fit of reciprocal lifetimes (corrected for the low-temperature contribution) to the Arrhenius equation gave estimated room temperature phosphorescence lifetimes of a few nanoseconds, consistent with the failure to observe room temperature emission. Fitting of the nonlinearity of the data seen in these plots suggested that two high-temperature processes were occurring with estimated activation parameters (E in kJ mol^{-1} and A in s^{-1}) for $Cr([18]\text{-}aneN_6)^{3+}$: $E_1 = 40$, $A_1 = 1 \times 10^{16}$; $E_2 = 24$, $A_2 = 1 \times 10^{14}$: $Cr(sen)^{3+}$; $E_1 = 45$, $A_1 = 2 \times 10^{15}$; $E_2 = 29$, $A_2 = 7 \times 10^{11}$. $Cr([18]\text{-}aneN_6)^{3+}$ was photochemically inert on irradiation. On irradiation into the lowest quartet ligand field absorption band, $Cr(sen)^{3+}$ photolyzes with a quantum yield of 0.098 ± 0.001 at room temperature. Laser flash photolysis with conductivity detection showed that this photoreaction occurred faster than protonation of the liberated amine ligand at all practical proton concentrations. The quantum yield for irradiation directly into the doublet absorption band of $Cr(sen)^{3+}$ was 0.077 ± 0.003. Photoaquation of Δ-$Cr(sen)^{3+}$ led to loss of optical activity and product analysis by capillary electrophoresis showed that both racemic and Δ-$Cr(sen)^{3+}$ photoaquate to a single main product, *trans*-$Cr(sen\text{-}NH)(H_2O)^{4+}$. The product stereochemistry is shown to be consistent with predictions based on the angular overlap model for Cr(III) photochemistry, recognizing the additional constraints imposed by the ligand. The abnormally short room temperature solution lifetime of the doublet state is a result of a radiationless process that competes with other processes depleting the doublet state. However, this doublet-state deactivation process does not lead to photoaquation but competes with BISC and photoaquation via the quartet state, resulting in an unprecedented reduction in photoaquation quantum yield on direct irradiation into the doublet state.

Introduction

The availability of macrocyclic complexes has permitted useful explorations of the effect of ligand constraints on photochemical pathways and quantum yields. Early work by Kutal,[1,2] Kane-Maguire,[3,4] and co-workers showed that a number of Cr(III) *trans*-cyclam complexes were photoinert, and this was attributed to the effect of steric rigidity on access to the photochemical channels of excited-state decay. In other studies it has been found[5,6] that reaction pathways can be modified by steric factors associated with the presence of multidentate ligands. This area has advanced sufficiently to

* To whom correspondence should be addressed. E-mail: kirkad@uvic.ca.
† University of Victoria.
‡ Southern Alberta Institute of Technology.

(1) Kutal, C.; Adamson, A. W. *J. Am. Chem. Soc.* **1971**, *93*, 5581−2.
(2) Kutal, C.; Adamson, A. W. *Inorg. Chem.* **1973**, *12*, 1990−4.
(3) Kane-Maguire, N. A. P.; Wallace, K. C.; Miller, D. *Inorg. Chem.* **1985**, *24*, 597−605.
(4) Kane-Maguire, N. A. P.; Wallace, K. C.; Speece, D. G. *Inorg. Chem.* **1986**, *25*, 4650−4.
(5) Saliby, M. S.; Sheridan, P. S.; Madan, S. K. *Inorg. Chem.* **1980**, *19*, 1291−7.
(6) Kirk, A. D.; Namasivayam, C.; Ward, T. *Inorg. Chem.* **1986**, *25*, 2225−9.

10.1021/ic010236j CCC: $22.00
Published on Web 01/26/2002

hold out promise that such effects of ligand constraints may be usefully employed to alter and control photochemical behavior including the ability to design photochemically inert, luminescent complexes.

As one aspect of these studies, Endicott and co-workers have reported on some interesting examples[7−17] of complexes that show large and puzzling variations in their emission lifetimes and quantum yields in room temperature aqueous solutions. One particularly interesting example[15] is the molecule $Cr(sen)^{3+}$, a complex analogous to $Cr(en)_3^{3+}$ but in which three of the nitrogen coordinators are required to remain in a facial configuration by a neopentyl cap. It was reported that this molecule had an unusually short emission lifetime in room temperature aqueous solution. This was attributed to the operation in the doublet excited state of a very rapid radiationless decay to the ground state, a process induced by a relaxation of the ligand strain which results from the twist angles imposed on the ligand by coordination. At the same time, the molecule was reported to photoaquate, but no data revealing the pathway of this photochemistry were reported. Because of our interest in this latter aspect and to further explore the nature of the excited states leading to photoaquation, we have undertaken a more detailed investigation of the photochemical pathway for this molecule. We have also been able to compare the photophysics of this photoactive nonemissive system to that of a photoinert, nonemissive system,[18] $(Cr([18]\text{-}aneN_6)^{3+}$, where the ligand is a macrocycle having all of the six secondary nitrogen coordinators separated by two methylene groups. Along with a study of the photostereochemistry of $Cr(sen)^{3+}$, the results are reported here.

Experimental Section

Syntheses and Crystal Growth. $[Cr([18]\text{-}aneN_6)]Br_3$. The salt $[18]\text{-}aneN_6{\cdot}3H_2SO_4$ (Aldrich) was dissolved in water and made basic (pH ∼ 13) with 2 M sodium hydroxide solution. By continuously extracting the aqueous solution with chloroform, the free ligand was obtained as a colorless solid. $CrCl_3{\cdot}6H_2O$ (0.124 g, 0.5 mmol) was dissolved in 20 mL of dimethyl sulfoxide (dmso) at 190 °C. The volume of the solution was reduced to ∼10 mL, and a 0.5 mmol (0.134 g) solution of the free ligand in ethanol (5 mL) was added to the cooled metal containing solution at 60 °C. The temperature was raised slowly to 170 °C during which time a yellow precipitate formed. Stirring was continued for 1 h at 170 °C after which the yellow solid was filtered off and washed with ethanol and ether. After air-drying, it was redissolved in water (∼4 mL) at 50 °C and 2 mL of a saturated solution of sodium bromide was added. Yellow crystals were obtained on slow evaporation. The crystals were filtered off and dried under vacuum (yield: 0.28 g; 0.35 mmol; 70%). Anal (calcd (%), found (%)) for $[Cr(C_{12}H_{30}N_6)]Br_3$: C, 26.19, 26.20; H, 5.49, 5.44; N, 15.27, 15.25. UV/vis (H_2O; obsd λ (ϵ), lit.[18] λ (ϵ)): 468 (227), 466 (227); 366 (92), 361 (103).

$[Cr(sen)]Br_3$ was synthesized in a procedure analogous to the above from the ligand 4,4′,4″-ethylidyne tris(3-azabutan-1-amine) which was prepared following a literature procedure.[19] This gave yellow crystals of $[Cr(sen)]Br_3$ in 75% yield. Anal (calcd (%), found (%)) for $[Cr(C_{11}H_{30}N_6)]Br_3$: C, 24.55, 24.50; H, 5.58, 5.62; N, 15.62, 15.74. UV/vis (H_2O; obsd λ (ϵ), lit.15 λ (ϵ)): 452 (93), 451 (97); 349 (63), 347 (65).

The perchlorate and chloride salts of $Cr(sen)^{3+}$ were obtained by recrystallization of the bromide salt in the presence of an excess of the lithium or sodium salt of the desired anion. $(+)_D$-$[Cr(sen)]Cl_3$ was obtained as the less soluble salt from selective crystallization of the D-tartrate diastereoisomers as described[20] in the literature for $Cr(en)_3^{3+}$, for which the $(+)_D$-$[Cr(en)_3]Cl_3$ form, $[\alpha]_D = 103°$, was assigned the D configuration. For $(+)_D$-$[Cr(sen)]Cl_3$, $[\alpha]_D = 43°$; details of the optical rotation at other wavelengths have been published.[21] Preparation of the $(-)_D$-$[Cr(sen)]Cl_3$ enantiomer using L-tartaric acid was less successful, producing material with $[\alpha]_D = -22°$, but this material was still useful for checking chromatographic and capillary electrophoretic separations and retention times.

UV−Vis Spectra. UV−vis spectra were run on a Philips PU 8740 UV−vis spectrophotometer using 1 cm quartz cells or a Cary 5 UV−vis−near-IR spectrophotometer using a 10 cm quartz cell. Solutions used were micropore filtered using 0.22 μm filters to reduce scattering.

Emission Spectra and Lifetimes. Steady-state emission spectral measurements were made using light from a Hanovia xenon lamp filtered by a combination of a Bausch and Lomb monochromator with an infrared filter (Balzers). Emission was detected by using a Jarrel-Ash 0.25 m monochromator preceded by a Corning 3-71 red filter and a concentrated potassium dichromate solution of 1 cm path length to remove light of wavelengths shorter than about 650 nm. The detector was an RCA 31034 photomultiplier with a modified Keithley 410 electrometer. Emission lifetimes were measured by using a PTI PL 2300 nitrogen laser for excitation and following the emission decay using a Jarrel-Ash monochromator/optical filter/Hamamatsu R928 photomultiplier/Tektronik 2230 oscilloscope combination with a GPIB interface to an ATARI 1040 computer. Lifetimes were evaluated by weighted linear regression[22] on log(intensity) versus time plots over 1024 channels of decay. Low-temperature emission lifetimes were measured in a dmso/H_2O glassy medium initially at 77 K, which was then allowed to slowly warm (2 h) to 0 °C. While lifetime measurements were taken, temperatures were continuously monitored using a Perkin-Elmer Coleman 165 chart recorder with a chromel/alumel thermocouple embedded in the sample.

(7) Ramasami, T.; Endicott, J. F.; Brubaker, G. R. *J. Phys. Chem.* **1983**, *87*, 5057−9.
(8) Endicott, J. F.; Tamilarasan, R.; Lessard, R. B. *Chem. Phys. Lett.* **1984**, *112*, 381−6.
(9) Endicott, J. F.; Lessard, R. B.; Lei, Y.; Ryu, C. K.; Tamilarasan, R. *ACS Symp. Ser.* **1986**, *307*, 85−103.
(10) Endicott, J. F.; Ramasami, T.; Tamilarasan, R.; Lessard, R. B.; Chong, K. R.; Brubaker, G. R. *Coord. Chem. Rev.* **1987**, *77*, 1−87.
(11) Lessard, R. B.; Endicott, J. F.; Perkovic, M. W.; Ochrymowycz, L. A. *Inorg. Chem.* **1989**, *28*, 2574−83.
(12) Ryu, C. K.; Lessard, R. B.; Lynch, D.; Endicott, J. F. *J. Phys. Chem.* **1989**, *93*, 1752−9.
(13) Endicott, J. F.; Lessard, R. B.; Lynch, D.; Perkovic, M. W.; Ryu, C. K. *Coord. Chem. Rev.* **1990**, *97*, 65−79.
(14) Perkovic, M. W.; Endicott, J. F. *J. Phys. Chem.* **1990**, *94*, 1217−19.
(15) Perkovic, M. W.; Heeg, M. J.; Endicott, J. F. *Inorg. Chem.* **1991**, *30*, 3140−7.
(16) Lessard, R. B.; Heeg, M. J.; Buranda, T.; Perkovic, M. W.; Schwarz, C. L.; Yang, R.; Endicott, J. F. *Inorg. Chem.* **1992**, *31*, 3091−103.
(17) Endicott, J. F.; Perkovic, M. W.; Heeg, M. J.; Ryu, C. K.; Thompson, D. *Adv. Chem. Ser.* **1997**, *253*, 199−220.
(18) Chandrasekhar, S.; Fortier, D. G.; McAuley, A. *Inorg. Chem.* **1993**, *32*, 1424−1429.
(19) Geue, R. J.; Searle, G. H. *Austr. J. Chem.* **1983**, *36*, 927−935.
(20) Galsbol, F. *Inorg. Synth.* **1970**, *12*, 274.
(21) Mackay, I. Ph.D. Dissertation, University of Victoria, 1998.
(22) Demas, J. N. *Excited-State Lifetime Measurements*; Academic Press: New York, 1983.

Quantum Yield Determinations. Radiation at 436 nm from a 100 W mercury lamp was passed through a Corning CS 7-60 filter and a 5 cm water filter to remove the infrared components. The lamp intensity was in the range $(1-10) \times 10^{-8}$ einstein s^{-1} as measured by ferrioxalate actinometry.[23,24] Efficiently stirred solutions with 3.8×10^{-3} M concentration of metal complex at pH 3.0 were irradiated in 1 cm cuvettes at 20 °C, and the pH was monitored by an Ingold LOT combination electrode interfaced to a PDP-11 computer. Standard acid (0.094 27 M $HClO_4$) was added from a 200 μL stepping motor buret, resolution 0.05 μL, under program control in order to maintain constant solution pH and a record kept of the volume of acid added versus time before, during and after photolysis. To avoid problems with secondary photolysis, the solutions were photolyzed to less than 5% conversion. Quantum yields at 514 nm were measured in the same way on pH 3.0 solutions with 1.0×10^{-4} M metal complex but using 60 mW (Scientech 365 digital power meter) of argon ion laser radiation expanded to 6 mm beam width. The photon flux into the sample was calculated from the power reading, irradiation wavelength and sample absorbance, correcting for window reflections.

For quantum yields at 675 nm (514.5 nm Coherent laser pumping at 2 W, Coherent Radiation Model 590 dye laser with birefringent tuning filter, line width 0.25 nm, rhodamine 640 dye, no beam expander) the radiation was passed through a 10.3 cm path length, 3 mm i.d. thermostated flow cell. The irradiation powers were in the range 20−40 mW. By using a peristaltic pump, the $Cr(sen)^{3+}$ solution, pH 3.0 and 4.0×10^{-2} M in complex was circulated through the photolysis cell and an external compartment containing the pH electrode and the stepper motor buret for acid addition. The pH-stat method described above was used to measure the proton uptake before, during, and after irradiation. In all the above quantum yield measurements, constancy of light flux throughout the experiments was confirmed by continuously monitoring the 8% of the beam reflected by a 45° silica window to a silicon photodiode/digital picoammeter.

Flash Photolysis. Nanosecond flash photolysis was carried out using a Spectra Physics Quanta-Ray GCR-11 Neodymium-YAG laser (≤50 mJ pulse energy, 5−6 ns pulse-width, 1 pulse s^{-1} at 355 nm). About 50 mL of a 1×10^{-3} M complex solution was flowed through a quartz cell ($0.7 \times 0.7 \times 0.3$ cm) using a peristaltic pump. A DC pulse detection system[25] was used to measure the conductivity changes upon irradiation.

Product Analysis. A Varian 5000 liquid chromatograph with a 25 cm octadecylsilane RP-HPLC column was employed to separate cationic mixtures by ion interaction chromatography. Eluents consisted of 25 mM tetraethylammonium ion as the competing cation, 25 mM hexanesulfonate as the anion interaction agent, and 50 mM of the chiral resolving agent D-tartaric acid. Eluents were made up with a mixture of 7.5% methanol (HPLC grade) in organo pure water. The pH of the solution was adjusted to ~3.6 by adding either base (NaOH) or additional D-tartaric acid. A flow rate of 1.5 mL/min was used, and peaks were detected by UV absorption at a wavelength of 250 nm using a Vari-Chrom variable wavelength detector.

An Applied Biosystems 270A-HT capillary electrophoremeter was used with a 50 μm capillary of 45 cm length and the injector separated by 27 cm from the UV−vis detector. Electropherograms were recorded using a Shimadzu C-R5A Chromatopac integrator. Migration times were reproducible within ±1% on a given day but, due to changes in capillary properties, displayed a larger drift over several days. The electrophoresis buffers were typically aqueous 50 mM D-tartaric acid solutions adjusted to pH 3.0−5.0 through the addition of NaOH or TRIS base. Usually the buffers were 4.0 mM in DETA (diethylenetriamine), an electroosmotic flow inhibitor.

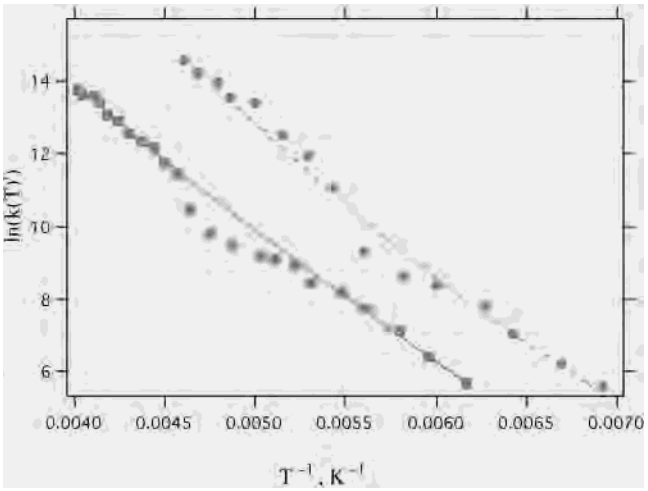

Figure 1. Plot of $\ln(k'(T))$ versus T^{-1} for $Cr([18]\text{-}aneN_6)^{3+}$ and $Cr(sen)^{3+}$. Rate constants in 1:1 dmso/water medium, $k'(T)$, corrected for low-temperature radiationless decay contribution are shown as $Cr([18]\text{-}aneN_6)^{3+}$: solid circles, $Cr(sen)^{3+}$ solid squares. The fits to the equation $A_1 \exp(-E_{a1}/RT) + A_2 \exp(-E_{a2}/RT)$, are shown as the dashed and solid lines, respectively.

Polarimetry. Optical rotations $[\alpha]_\lambda$ were measured at $\lambda = 365$, 405, 435, 546, 589, and 633 nm using a Rudolph Research Autopol III automatic polarimeter with a micropolarimeter cell of 10 cm path length and 2.0 mL volume.

Results

Emission Studies. Both $Cr([18]\text{-}aneN_6)^{3+}$ and $Cr(sen)^{3+}$ failed to show emission from room temperature aqueous solutions. At 77 K, $Cr([18]\text{-}aneN_6)^{3+}$ and $Cr(sen)^{3+}$ showed emission peaks at 692 and 676 nm, respectively. The $Cr([18]\text{-}aneN_6)^{3+}$ emission lifetime at 77 K in dmso/water glass was 162 μs and decreased with increasing temperature, showing the usual low- and high-temperature regimes. A single-exponential fit to the high-temperature region gave an apparent activation energy of 34.2 kJ mol^{-1}, which extrapolated to a predicted 293 K lifetime of 3 ns. This short lifetime is consistent with our inability to observe the resultant weak room temperature emission. For $Cr(sen)^{3+}$ the 77 K dmso/water glass lifetime was 157 μs with an apparent activation energy for the high-temperature regime of 33.9 kJ mol^{-1} and a predicted 293 K lifetime of 2 ns, results consistent with earlier reports.[15] These behaviors contrast with that of $Cr(en)_3^{3+}$ with its 77 K dmso/water glass lifetime of 120 μs, single apparent higher temperature activation energy of 46 kJ mol^{-1}, and room temperature lifetime of 1.6 μs.

More detailed analysis of the high-temperature behavior gave the results observed in Figure 1 for the high-temperature regime with the low-temperature decay rate subtracted out. Whereas the $Cr(en)_3^{3+}$ reciprocal lifetimes corrected for the low-temperature contribution gave a linear fit to a single exponential, the data for $Cr([18]\text{-}aneN_6)^{3+}$ and $Cr(sen)^{3+}$

(23) Hatchard, C. G.; Parker, C. A. *Proc. R. Soc. (London) A* **1956**, *235*, 518.
(24) Kirk, A. D.; Namasivayam, C. *Anal. Chem.* **1983**, *55*, 2428−9.
(25) Irwin, G. Ph.D. Dissertation, University of Victoria, 1999.

required a double exponential function to fit the curvature seen in the high-temperature lifetimes. As clearly shown in Figure 1, both complexes display a "kink" in the temperature data of the type reported by others and attributed either to competition between internal and solvent relaxation processes[26] or to a glass transition.[10] The data were fit to a double-exponential function using the proprietary nonlinear least squares routine of Igor Pro(Wavemetrics). The covariance matrix indicated that the uncertainties in the best fit were large and that the A and E values resulting were significantly correlated. Nevertheless reasonable fits, shown in Figure 1, were obtained with the values (E in kJ mol^{-1} and A in s^{-1}) for Cr([18]-aneN$_6$)$^{3+}$: $E_1 = 40$, $A_1 = 1 \times 10^{16}$; $E_2 = 24$, $A_2 = 1 \times 10^{11}$. The values for Cr(sen)$^{3+}$ are as follows: $E_1 = 45$, $A_1 = 2 \times 10^{15}$; $E_2 = 29$, $A_2 = 7 \times 10^{11}$.

Photolysis Processes. Flash photolysis of Cr([18]-aneN$_6$)$^{3+}$ in 1×10^{-3} M $HClO_4$ did not result in any measurable permanent conductivity change. This was consistent with the observed absence of any proton uptake on conventional photolysis at 436 nm and confirms that the complex is inert to photoaquation of amine ligands.

Flash photolysis of Cr(sen)$^{3+}$ in various $HClO_4$ solutions gave an exponential conductivity decrease corresponding to proton uptake, but the observed lifetime for the conductivity change was found to be linearly dependent on the concentration of the acid present. The proton concentration was increased from 1×10^{-3} to 4×10^{-3} M, the upper limit fixed by the maximum current rating of the conductivity pulser, and the observed lifetime decreased from 524 to 163 ns. This indicates that the protonation of the liberated amine ligand is the rate-limiting process and that the photoreaction is occurring on a shorter time scale. A plot of reciprocal lifetime versus proton concentration was linear giving a protonation rate constant of 1.4×10^9 M^{-1} s^{-1}. Protonation rate constants for other liberated amine groups range[27] from 0.3×10^{10} to 2×10^{10} M^{-1} s^{-1}, so this value for Cr(sen)$^{3+}$ value is beyond the low end of the range. The lowest literature rate constant, 3×10^9 M^{-1} s^{-1}, was for the complex Cr(en)$_3$$^{3+}$ and suggests that lower protonation rate constants are to be expected for complexes containing multidentate ligands. This would be expected as photoliberated amines remain tethered to the metal center in the photoproduct for these complexes and therefore encounter greater steric hindrance toward protonation.

Conventional photolysis of Cr(sen)$^{3+}$ at 436 nm led to nonlinear proton uptake. The time dependence of the volume of acid added was therefore fitted to a quadratic in time and the initial slope used to calculate the quantum yield of proton uptake, yielding the result 0.10 ± 0.01 based on six measurements, in excellent agreement with the literature value.[15]

Quantum yields on irradiation into the quartet and doublet states were measured by laser irradiation at 514 and 675 nm, respectively. A typical 675 nm result is shown in Figure 2; the inset to the figure shows the absorption spectrum of Cr(sen)$^{3+}$ in the doublet region and its relation to the quartet absorption bands. The proton uptake was linear during photolysis, and both pre- and postphotolysis proton uptakes were negligible, allowing easy determination of the extent of photoreaction. The results and calculated quantum yields are summarized in Table 1, which shows overall quantum yields for proton uptake of 0.098 ± 0.001 at 514 nm and 0.077 ± 0.003 at 675 nm. Since wavelength dependence of the quantum yield on irradiation into the quartet state would be unusual in a complex of this type, the observation that the quantum yield at 514 nm is essentially the same as that measured at 436 nm precludes any significant systematic errors. This also provides reassurance as to the accuracy of the digital power meter as well as the procedures used for power measurement and corrections for window reflections, etc.

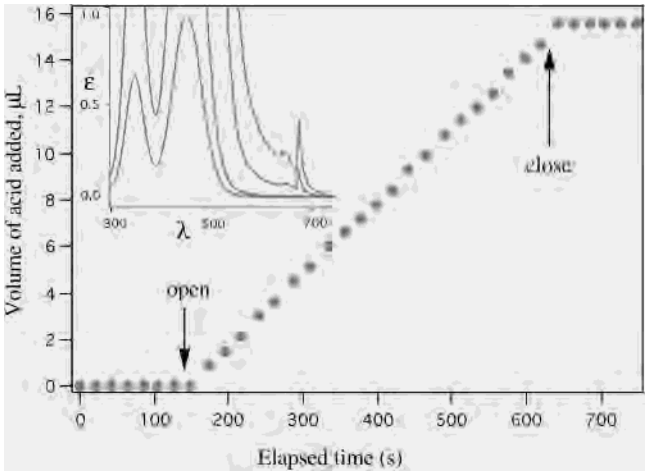

Figure 2. Proton uptake during photolysis at 675 nm of Cr(sen)$^{3+}$ in 1.0×10^{-3} M $HClO_4$: *Y*-axis, volume of 0.1 M acid added to maintain pH constant; *X*-axis, elapsed time. Vertical arrows show times at which beam shutter was opened and closed. The inset shows the absorption spectrum of Cr(sen)$^{3+}$ in the doublet and quartet bands; the doublet absorption maximum is at 675 nm.

The lower yield observed at 675 nm is statistically significant since the quantum yield difference between the two wavelengths 514 and 675 nm is more than 10 times the pooled standard deviation. However, systematic errors could also be important. First, for the doublet irradiation experiment there could be a small mismatch between the doublet absorption wavelength measured on a spectrophotometer and the dye laser wavelength, calibrated using a monochromator. The doublet absorption is only about 5 nm half-width, while the dye laser line width is specified as 0.25 nm. However, if the laser is not precisely centered on the absorption, an apparently low quantum yield will result. To avoid this error, the apparent quantum yield was measured for a range of birefringent filter settings around the nominal setting for 675 nm with the result shown in Figure 3, and the quantum yield measurements reported were then made at the micrometer setting that gave the maximum quantum yield value. The second possibility is a wavelength dependence of the power meter reading. However, the device is a bolometer, which depends on the heat supplied by the incident light to a black thermal sensor. For this reason it is most unlikely that this power reading would show any significant wavelength

(26) Forster, L. S. *Inorg. Chim. Acta* **1998**, *277*, 211−218.
(27) Waltz, W. L.; Lilie, J.; Lee, S. H. *Inorg. Chem.* **1984**, *23*, 1768−75.

Table 1. Proton Uptake Quantum Yields for $Cr(sen)^{3+}$ at 295 K

irradiation wavelength (nm)	absorbance (mW of incident light)	irradiation time (s)	μL 0.094 27 M acid added	quantum yield	mean and std dev
514	0.05/60.0	160	4.5	0.0983	
514	0.05/60.0	176	4.9	0.0973	
514	0.05/60.0	160	4.5	0.0983	
514	0.05/60.0	183	5.2	0.0993	
514	0.05/60.0	168	4.7	0.0978	
					0.098 ± 0.001
675	0.18/33.0	570	27.6	0.0753	
675	0.036/26.0	1221	11.40	0.0786	
675	0.090/22	1227	23.8	0.0820	
675	0.18/27.5	554	22.8	0.0768	
675	0.18/27.5	554	22.0	0.0741	
					0.077 ± 0.003

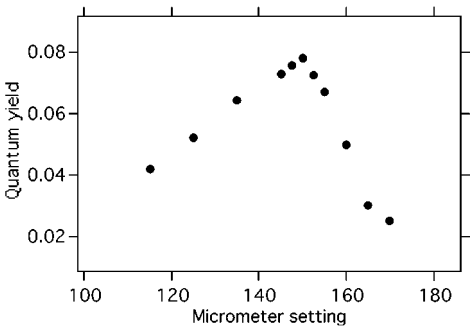

Figure 3. Plot of observed $Cr(sen)^{3+}$ photoaquation quantum yield on direct irradiation into the doublet state versus micrometer setting on the dye laser birefringent filter.

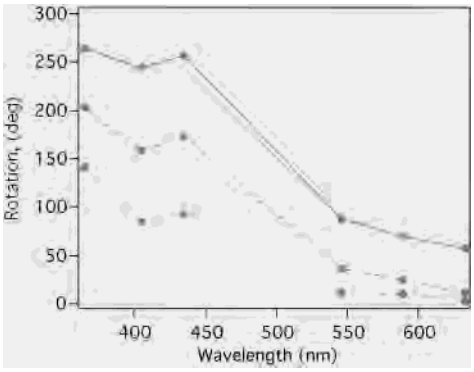

Figure 4. Changes in optical rotation of Δ-$[Cr(sen)]Cl_3$ (1.0×10^{-2} M in 0.010 M $HClO_4$. Photolysis: 50 mW at 488 nm; solid line, 0 min; dashed line, 10 min; dotted line, 20 min. Measurements at 365, 405, 435, 546, 589, and 633 nm.

dependence. Supporting this is the manufacturer's specification claiming less than 3% variation in detector response over a much wider wavelength range than was used in this work. We therefore conclude that the yield on doublet irradiation is genuinely lower than that observed for quartet irradiation.

Photoproduct Studies. On laser irradiation of $Cr(sen)^{3+}$ at 488 or 458 nm, the UV/vis spectrum showed changes consistent with production of photoproducts with red-shifted ligand field maxima. Specifically these were consistent with expectations for substitution of an amine ligand by water and further supported by the proton uptake observed on photolysis. Figure 4 shows the results obtained on measurement of the optical rotation of a solution of resolved $Cr(sen)^{3+}$ as a function of photolysis time. At all wavelengths examined, there was a decrease in optical rotation proportional to photolysis time. In contrast to this, the complex was thermally stable, showing no rotation changes under the conditions of low pH, temperature, and time used in the photolysis experiments.

In initial studies,[21,28] HPLC analysis indicated that several photoproducts were formed. More recent analyses using capillary electrophoresis (CE), which gives superior separations, have shown those results to be distorted by interfering chloride or bromide anation processes. The CE studies also revealed that the importance of the anation relative to aquation was enhanced in the HPLC work by the necessity to analyze the peaks at 250 nm because of the UV absorption of the methanol component of the HPLC eluent at shorter wavelengths. At 250 nm the relative UV absorption of the anation products is very significantly stronger than that of the aquated products, causing the minor artifact peaks to dominate in the chromatogram and leading to the earlier confusing and incorrect findings. The aqueous buffer used in the CE method permits analysis at 210 nm where there exists higher relative sensitivity for the aquation products. Use of the perchlorate salt precludes any possibility of anation, although we found that, with CE analysis at 210 nm, comparable results were obtained with either perchlorate or halide salts. The results reported here therefore supersede the earlier reports.[21,28]

Photolysis of 5.0×10^{-3} M *rac*-$[Cr(sen)](ClO_4)_3$ and Λ-$[Cr(sen)]Br_3$ solutions in 1×10^{-3} M $HClO_4$ with 30 mW of 458 nm radiation, followed by CE analysis, gave the results shown in Figure 5A,B, respectively. Figure 5A shows that the Λ- and Δ-$Cr(sen)^{3+}$ enantiomers were almost baseline separated, migrating at 10.3 and 10.5 min, respectively. Figure 5B shows that a small amount of the Δ-isomer was present in Λ-$[Cr(sen)]Br_3$. Photolysis of these solutions resulted in the same two product peaks, a main sharp peak migrating at 12.2 min and a minor broad, indistinct but reproducible peak following this at 13 min.

As a step toward identification of these product peaks, the electropherograms were obtained for the thermolysis of *rac*- and Λ-$[Cr(sen)](ClO_4)_3$. To get any appreciable thermal product, the solutions had to be heated to reflux temperatures. The results are shown in Figure 6A,B, respectively. These show the same major product as the photolysis experiments but no evidence of the broad peak. A new small, sharper peak did grow in at 14 min. An interesting feature of the

(28) Kirk, A. D. *Chem. Rev.* **1999**, *99*, 1607−40.

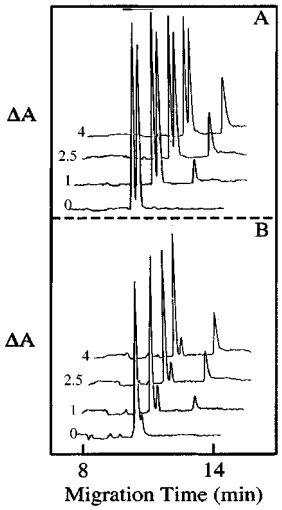

Figure 5. Photoaquation product analysis by capillary electrophoresis: (A) *rac*-[Cr(sen)]$(ClO_4)_3$; (B) Λ-[Cr(sen)]Br_3. Complexes 5.0 mM in 1×10^{-3} M $HClO_4$. Electropherograms are shown diagonally offset for progressively increasing photolysis times, with 50 mW of light at 488 nm, of 0, 1, 2.5, and 4 min, respectively, as shown at the start of each curve. Major peaks are, in migration sequence, Λ-$Cr(sen)^{3+}$, Δ-$Cr(sen)^{3+}$, and photoproduct. CE conditions: buffer, 50 mM D-tartrate with 4.0 mM diethylenetriamine adjusted to pH 5.0; applied voltage, 10 kV; detection wavelength, 210 nm; capillary length, 45 cm; distance to detector, 27 cm.

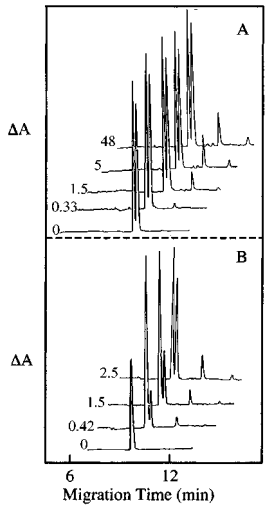

Figure 6. Thermal aquation product analysis by capillary electrophoresis: (A) *rac*-[Cr(sen)]$(ClO_4)_3$; (B) Λ-[Cr(sen)]Br_3. Complexes 5.0 mM in 1×10^{-3} M $HClO_4$. Electropherograms are shown diagonally offset for increasing thermal reaction times at the solution normal boiling point. Times are 0, 0.33, 1.5, 5, and 48 h, respectively, in A and 0, 0.42, 1.5, and 2.5 h, respectively, in B as shown at the start of each curve. CE conditions as in Figure 5.

thermolysis of Λ-[Cr(sen)]$(ClO_4)_3$ was that Δ-[Cr(sen)]-$(ClO_4)_3$ grew in as the thermolysis progressed. Racemization was efficient, resulting in a near-racemic mixture after about 2.5 h of refluxing and complete racemization within 48 h. The results presented in Figure 6A show the data for *rac*-[Cr(sen)]$(ClO_4)_3$ also to 48 h; both solutions showed no further changes after continuous reflux for a week. This indicated that an equilibrium composition had been reached and also demonstrates the remarkable resistance of $Cr(sen)^{3+}$ to hydrolysis in acidic solution.

As a further step toward product identification, Figure 7 compares the photoproducts obtained from solutions of

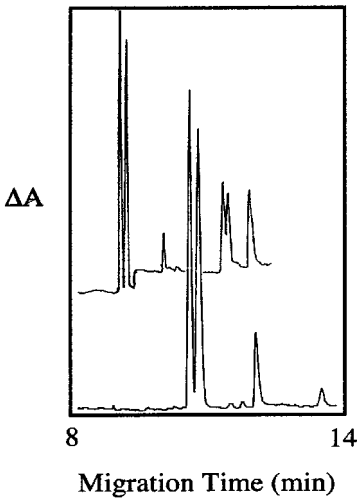

Figure 7. Comparison of the CE migration behavior of the photoaquation products of *rac*-$Cr(en)_3^{3+}$, upper trace, with the products of the 48 h thermal aquation of *rac*-$Cr(sen)^{3+}$, lower trace. CE conditions as in Figure 5.

Λ-[Cr(sen)]$(ClO_4)_3$ with those from Δ-[Cr(en)$_3$]$(ClO_4)_3$ which have earlier been identified[29] as 28% Δ-*cis*-$Cr(en)_2$-(en-H)$(OH_2)^{4+}$, 7% Λ-*cis*-$Cr(en)_2$(en-H)$(OH_2)^{4+}$, and 65% *trans*-$Cr(en)_2$(en-H)$(OH_2)^{4+}$.

Discussion

In a series of papers, Endicott and co-workers have presented data on doublet-state relaxation processes in a variety of Cr(III) complexes containing ligands that impose distorted or strained coordination environments on the metal center. Several of these molecules have unusually short phosphorescence decay lifetimes in aqueous room temperature solution, and these have been attributed to a rapid relaxation process that depopulates the doublet state. In a recent review Endicott summarizes[17] these studies, claiming that this thermally activated relaxation process involves a quenching channel for which the critical nuclear coordinate is a trigonal twist. This conclusion was supported by MM2 calculations. These show that, for a series of complexes, there is a correlation between the rate constant for relaxation and the change in the steric energies of the respective ligands when they are twisted around the C_3 axis by 15° relative to their configuration in the ground state of the complex. The major question that is addressed but not definitively answered in these papers is whether or not this relaxation pathway leads to chemical reaction such as photoaquation or photoisomerization in the molecules where it occurs. It was recognized that solvent association may play a role in facilitating the relaxation and hence lead to photoreaction where the ligand constraints permit this. In summary, the pathway of photochemistry in such complexes is not at all clear, and this was a major impetus for the present detailed study of $Cr(sen)^{3+}$.

The present study of the relaxation processes in the photoactive complex $Cr(sen)^{3+}$ supports the earlier reports[15] of a short doublet-state lifetime in room temperature aqueous solution, estimated by us as 2 ns at 295 K and by Endicott

(29) Cimolino, M. C.; Linck, R. G. *Inorg. Chem.* **1981**, *20*, 3499−503.

et al. as 0.1 ns at 298 K. What is interesting is that the photoinert $Cr([18]\text{-}aneN_6)^{3+}$ behaves in a similar fashion, having a doublet lifetime estimated from a single-exponential extrapolation as 3 ns at 295 K. These nanosecond values are remarkable when compared with the 1.6 ms doublet lifetime at 293 K of the analogous complex $Cr(en)_3^{3+}$. Even more striking is the detail of the lifetime behavior as a function of temperature. As detailed in Results, both complexes show nonlinear plots of logarithmic phosphorescence decay lifetime versus reciprocal temperature. After correction for the contribution of the low-temperature relaxation, the data can be fit in terms of two high-temperature processes, one with an apparent activation energy in excess of 40 kJ mol^{-1} and the other around 30 kJ mol^{-1}. The first of these apparent activation energies is typical of values observed in solution for complexes that apparently relax by back-intersystem crossing, such as[30] the 46 kJ mol^{-1} reported for $Cr(en)_3^{3+}$. The second is for the additional channel studied by Endicott et al. It is interesting to note that this apparent activation energy is of a magnitude similar to those reported[31] for some complexes with strong field ligands such as cyanide, in which it is presumed that relaxation by back-intersystem crossing is energetically impossible.

We therefore agree that there is a fast relaxation process in $Cr(sen)^{3+}$, but we note that we find a parallel phenomenon also in $Cr([18]\text{-}aneN_6)^{3+}$, a photoinert complex. The molecule $Cr([18]\text{-}aneN_6)^{3+}$ in the solid state has S_6 point group symmetry,[32] so the Kepert twist angle in the ground state is exactly 30°. Unless this point represents a maximum rather than a minimum in the ligand strain profile with C_3 twist angle, this does not seem consistent with a pathway that involves a relaxation via a trigonal twist of strain in the ground-state ligand conformation in the complex. It seems more likely that, in this complex at least, the faster radiationless decay process is a result of the distortion from octahedral geometry that exists in this molecule. This presumably leads to a mixing of states having doublet and quartet character and in consequence will serve to render ISC to the ground state less forbidden.

Irradiation of $Cr(sen)^{3+}$ into the lowest energy quartet state at 546 nm using a mercury lamp/interference filter as the light source was found to lead to photoaquation of an amine ligand and proton uptake with a quantum yield of 0.10 ± 0.01, in excellent agreement with the value reported earlier.[15] However, the interest here was not so much to confirm the earlier measurement but as a first step for exploring the nature of the excited-state participation in this photochemistry. A popular method used for this purpose has been via studies of the effect of doublet-state quenchers on the photochemical quantum yield and phosphorescence lifetime or intensity. For this complex, however, such an approach is infeasible due to the nanosecond doublet-state lifetime in room temperature aqueous solution. This implies a requirement to add quencher concentrations that are far too high to be practicable. We therefore undertook the much more difficult experiment of comparing the quantum yields of photoaquation on irradiation into the quartet and doublet states.

Such experiments are best carried out with laser light sources, making sure that the solution absorbances, etc., are the same or similar at both wavelengths used. It is also crucial to adjust the dye laser wavelength to the center of the narrow doublet absorption band and also to ensure that the absorbance at the maximum of the doublet absorption is measured with a spectrophotometer set to a sufficiently narrow bandwidth to avoid departure from Beer's law and to obtain the correct molar absorptivity. Light intensities were measured absolutely using a calibrated bolometer light meter and monitored continuously during photolysis using a silicon diode light meter, with corrections for window reflections. In these experiments we obtained a quantum yield for irradiation into the first quartet absorption band at 514 nm of 0.098 ± 0.001, in excellent agreement with the value measured at 546 nm conventionally with chemical actinometry. Parallel experiments using a dye laser with the wavelength carefully adjusted, Figure 3, to the maximum of the doublet absorption band at 675 nm gave the result $\phi_D = 0.077 \pm 0.003$.

Several studies of analogous complexes with six nitrogen coordination have found the same quantum yield on quartet and doublet irradiation. A few have reported higher quantum yields for irradiation directly into the doublet state, but to find a lower quantum yield on irradiation into the doublet is unprecedented. The question immediately arises as to whether this result may be the result of systematic errors. As detailed in Results, we have carefully checked for these and do not believe this to be the situation. We conclude the lower doublet quantum yield observed is genuine. Examination of the UV absorption spectrum in the doublet region shown in the inset to Figure 2 and published elsewhere[21] shows that up to about 20% of the absorption at 675 nm might be into the underlying tail of the quartet state. If this is so, then the true doublet quantum yield would be proportionately lower than 0.08.

What does this imply about the pathways of the photochemistry? Suppose the doublet-state or a ground-state intermediate derived from it were to be the exclusive precursor of reaction, possibly associated with the relaxation pathway proposed by Endicott and co-workers. Then, unless the intersystem crossing yield is unity, the quantum yield on irradiation into the doublet would have to be greater than or equal to that on irradiation into the quartet state. Such exclusive doublet reactivity is precluded by our results. Given the experience[28] that for other Cr(III) complexes with six nitrogen coordination (a) intersystem crossing yields are generally in the range of 0.7 to 0.8 and (b) the weight of evidence supports a back-ISC/quartet reaction pathway for the reaction via the doublet state, we are led to try to model the photochemistry of this complex using the general kinetic scheme[28] for quartet- and doublet-state processes. For simplicity we assume (a) that prompt ISC and prompt

(30) Lee, S. H.; Waltz, W. L.; Demmer, D. R.; Walters, R. T. *Inorg. Chem.* **1985**, *24*, 1531−8.
(31) Zinato, E. *Coord. Chem. Rev.* **1994**, *129*, 195−245.
(32) Chandrasekhar, S.; Fortier, D. G.; McAuley, A. *Inorg. Chem.* **1994**, *33*, 5610.

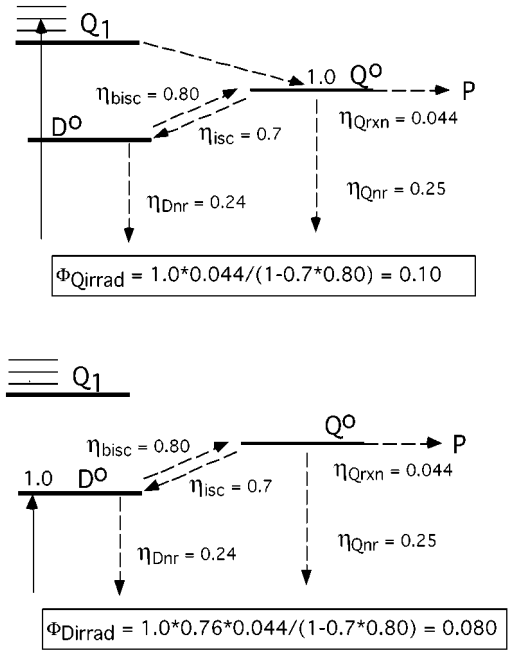

Figure 8. Proposed excited-state participation for $Cr(sen)^{3+}$. Upper half of diagram shows the pathway and calculation for the quartet irradiation quantum yield of 0.10. Lower part of diagram shows the pathway and calculation for the doublet irradiation quantum yield of 0.08.

reaction of the excited quartet states are unimportant and (b) that reaction occurs only via the relaxed quartet excited state.

Based on the published equations[28] for the quantum yield of various processes arising out of the quartet and doublet states, together with the simplifying assumptions mentioned above, the quantum yields observed on doublet and quartet irradiation can be used to estimate the efficiency of BISC as follows:

$$\phi_{\mathrm{Qirrad}} = \eta_{\mathrm{Qreacn}} + \eta_{\mathrm{ISC}}\eta_{\mathrm{BISC}}\eta_{\mathrm{Qreacn}}/(1 - \eta_{\mathrm{ISC}}\eta_{\mathrm{BISC}}) = \eta_{\mathrm{Qreacn}}/(1 - \eta_{\mathrm{ISC}}\eta_{\mathrm{BISC}}) = 0.098 \quad (1)$$

$$\phi_{\mathrm{Dirrad}} = \eta_{\mathrm{BISC}}\eta_{\mathrm{Qreacn}}/(1 - \eta_{\mathrm{ISC}}\eta_{\mathrm{BISC}}) = 0.077 \quad (2)$$

$$\phi_{\mathrm{Dirrad}}/\phi_{\mathrm{Qirrad}} = \eta_{\mathrm{BISC}} = 0.077/0.098 = 0.79 \quad (3)$$

In the above equations, η is the efficiency of a process, defined as the rate constant for a process involving an electronic state divided by the sum of the rate constants for all the processes occurring from that state. The subscripts signify the following: Qirrad and Dirrad = irradiation into the quartet and doublet states, respectively, ISC = intersystem crossing, BISC = back-ISC, Qreacn = reaction from the quartet state.

The quantum yields can be then be modeled by the BISC/quartet reaction model with the parameter values shown in Figure 8, where the 0.79 efficiency value for BISC has been rounded to 0.8 and the efficiency of ISC has been arbitrarily assumed to be 0.7, the same as for[27] $Cr(en)_3^{3+}$. Obviously this modeling is not unique but the correct quantum yields for doublet and quartet irradiation are predicted. Furthermore, the observed phosphorescence lifetime in solution in the high-temperature regime was described by a double exponential Arrhenius equation with order of magnitude A factors/activation energies of 2×10^{15} s^{-1}/45 kJ mol^{-1} and 7×10^{11} s^{-1}/29 kJ mol^{-1} for the two rate constants involved. The first set of parameters is consistent with expectations for BISC while the second set have a temperature coefficient of the order expected for doublet nonradiative decay (compare[33] $Cr(CN)_6^{3-}$). The large uncertainties in the derived Arrhenius parameters for the two processes in $Cr(sen)^{3+}$ preclude reliable calculation of $\eta_{\mathrm{BISC}} = k_{\mathrm{BISC}}/(k_{\mathrm{BISC}} + k_{\mathrm{Dnr}})$ at 295 K, but the implication is that it is less than unity, consistent with the photochemical results.

These results confirm that there is a rapid nonradiative decay process influencing the doublet lifetime in $Cr(sen)^{3+}$. However, it does not lead to, but competes with, reaction. Finally, the activation parameters for the process leading to reaction are consistent with expectations for the BISC/quartet reaction pathway. The nature of this radiationless process has been assigned as related to a trigonal twist resulting from ligand strain. This seems reasonable for $Cr(sen)^{3+}$, but we note that there is a parallel process occurring in $Cr([18]\text{-}aneN_6)^{3+}$ where the high symmetry of the coordinated ligand calls into question such an explanation.

Photostereochemistry. Assignment of the main product of the photoreaction as *trans*-$Cr(sen\text{-}NH)(H_2O)^{4+}$ can be based on the following observations. Here we choose sen-NH as the designation for a sen ligand with a dangling protonated arm, and sen-N for the un-protonated precursor. A single main product peak is observed in the photolysis of either *rac*- or Λ-complex, Figure 5. It follows that either this is the trans isomer or else the CE method is failing to separate the two enantiomers of a *cis*-$Cr(sen\text{-}NH)(H_2O)^{4+}$ photoproduct. Failure to resolve these product enantiomers is most unlikely as the enantiomers of the starting material are well separated and migrate before the photoproducts. The photoproducts are therefore expected to be better discriminated, not less. Consistent with this is the observation that the photoproduct enantiomers of $Cr(en)_3^{3+}$ are well separated under the same conditions; note also that the trans isomer elutes more slowly than the cis enantiomers (see Figure 7). Remember also that production of trans product in the photolysis is consistent with the loss of optical activity that was observed on photolysis, shown in Figure 4. The weight of this evidence favors *trans*-$Cr(sen\text{-}NH)(H_2O)^{4+}$ as the dominant photoproduct.

Our efforts to confirm this conclusion by analyzing the products obtained from thermolysis of $Cr(sen)^{3+}$ just complicated matters, however. On the basis of the stereoretentive thermal aquation behavior of Cr(III) complexes, the expectation was that thermolysis of Λ-, Δ-, or *rac*-$Cr(sen)^{3+}$ would give the respective *cis*-$Cr(sen\text{-}NH)(H_2O)^{4+}$ product(s). We should have then been able to prove directly that the two cis enantiomers were resolved from each other and from the trans isomer. Instead the thermal product analyses, shown in Figure 6, indicated that the same main product was formed from all three sources and moreover was the same as had been observed in the photolyses, Figure 5.

(33) Wasgestian, H. F. *Z. Phys. Chem.* **1969**, *67* (1−3), 39−50.

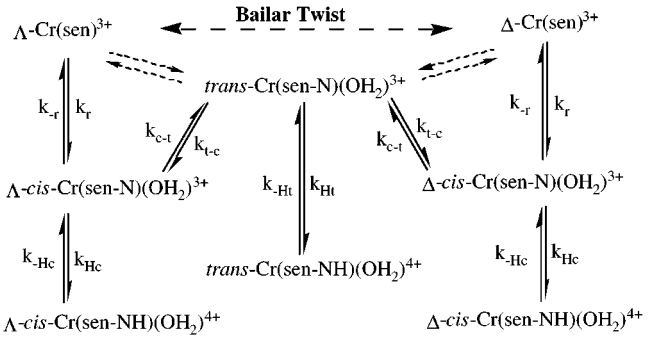

Figure 9. Thermal aquation and isomerization processes in $Cr(sen)^{3+}$.

This very unusual result may be partly a result of the fact that observation of any thermal aquation required refluxing the solutions for several hours. More importantly, it can be explained only if isomerization of initially generated *cis*-$Cr(sen\text{-}N)(H_2O)^{4+}$ occurs in competition with protonation and recyclization to $Cr(sen)^{3+}$, a process that may be quite rapid, leading to a low equilibrium concentration of the cis product. The resulting trans isomer cannot re-coordinate without prior deprotonation and isomerization, and this product may therefore be trapped and is observed in the product analysis. The observation that racemization occurs efficiently without any major build-up of other aquation products is consistent with such a mechanism for the thermal reaction and is encapsulated in Figure 9. For completeness the figure shows the possibility of racemization via a Bailar twist although we have no evidence bearing on the contribution of this pathway. In this figure it has also been shown, based on other recent studies[34] of the intermediates in Cr(III) photoreactions, that protonation plays an important role in the stabilization of monodentate aquated species. In further support of this mechanism is the observation, to be seen in Figure 7, that, in the equilibrium mixture obtained from thermal aquation of $Cr(sen)^{3+}$ at long reaction times, there are two small peaks migrating at the time expected for the cis isomers, just prior to the peak we have assigned as the trans isomer. Although not conclusive, the parallel with the behavior of $Cr(en)_3^{3+}$ also shown in Figure 7 is striking and supports the elution order, with D-tartrate medium, Δ-cis, Λ-cis, and trans for both of the $Cr(en)_2(en\text{-}NH)(H_2O)^{4+}$ and $Cr(sen\text{-}NH)(H_2O)^{4+}$ products.

We think it is also significant that the minor broad peak seen in the photoaquation data of Figure 5 is absent from all the $Cr(en)_3^{3+}$ analyses and from the $Cr(sen)^{3+}$ thermal reaction electropherograms, where the expectation is that only primary amine nitrogen coordination positions will be aquated. There is also no such peak in the photoaquation data for $Cr(en)_3^{3+}$. We conclude that this broad peak most likely corresponds to a small degree of photoaquation of a secondary amine nitrogen of the sen ligand. Our attempts to prove this by isolation of the resulting product were unsuccessful. Finally, in Figure 6, a small peak is to be seen for $Cr(sen)^{3+}$, migrating late at 14 min; this may correspond to thermal loss of a second primary amine of the ligand,

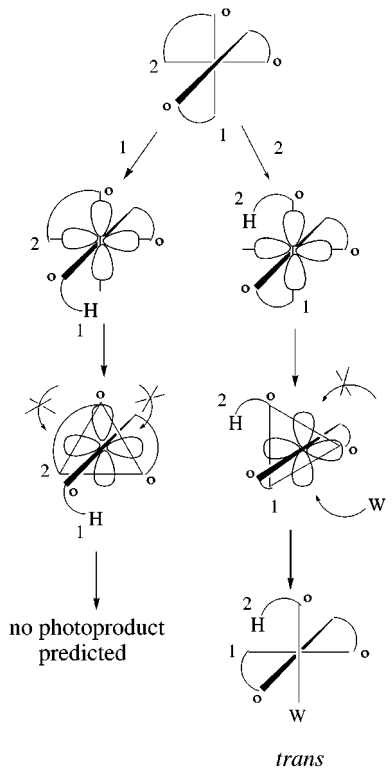

Figure 10. Angular overlap model symmetry rules and ligand constraints in the photoaquation of $Cr(sen)^{3+}$. The figure shows quartet-state excitation and ligand labilization in the plane of the paper. The neopentyl cap of the ligand restricts loss of secondary nitrogen ligands, marked with the secondary atom symbol "o", giving ligand nitrogens 1 and 2 as possible leaving groups. As shown in the left part of the diagram, trans attack of an entering water ligand on the N1 ligand is prevented by the steric constraints described in the discussion. The right part of the diagram shows the feasible ligand aquation of the N2 ligand that leads exclusively to the trans aquation product.

with formation of $Cr(sen(-NH)_2)(OH_2)_2^{5+}$ having two protonated dangling primary amine arms.

We now compare these conclusions to expectations based on the AOM theory[35−37] for d^3 complexes; we will use the simple pictorial versions[38,39] of the model discussed elsewhere. Figure 10 encapsulates the situation for Λ-$Cr(sen)^{3+}$. In the upper part of the figure we show the complex in its ground state with the nitrogen atoms bound to the neopentyl cap marked with the secondary atom symbol 'o'. Immediately below, left and right, is shown the complex in its quartet excited state with an e_g^* orbital occupied, here chosen as the orbital in the plane of the diagram. This labilizes the four coordinated nitrogen atoms in that plane, but two are secondary nitrogen ligands, constrained from leaving by the neopentyl cap. (This constraint may not be entirely effective as the product analysis of $Cr(sen)^{3+}$ indicates that photoaquation of a secondary amine may be a minor contributor as discussed above.) Now consider the remaining two nitrogen atoms labeled 1 and 2. The left side of the diagram

(34) Irwin, G.; Kirk, A. D. *Coord. Chem. Rev.* **2001**, *211*, 25−43.

(35) Vanquickenborne, L. G.; Ceulemans, A. *J. Am. Chem. Soc.* **1978**, *100*, 475−83.
(36) Vanquickenborne, L. G.; Ceulemans, A. *Coord. Chem. Rev.* **1983**, *48*, 157−202.
(37) Ceulemans, A. *NATO ASI Ser., Ser. C* **1989**, *288*, 221−54.
(38) Kirk, A. D. *J. Chem. Educ.* **1983**, *60*, 843−52.
(39) Kirk, A. D. *Comments Inorg. Chem.* **1993**, *14*, 89−121.

shows that loss of N1 would lead to a trigonal bipyramidal intermediate (tbp) in which the two equatorial edges favorable for ligand entry in the AOM model are subject to constraints on water entry. One is blocked by a ligand arm, while the other is flanked by two secondary nitrogen atoms that, together with the third, are required to remain *facial*. The AOM reaction pathway would require them to be *meridional* in the hypothetical product. Thus the combination of the symmetry rules and ligand constraints prevents net reaction by this left-hand pathway.

The right side of the diagram shows that loss of N2 leads to a tbp intermediate in which water entry at one symmetry-allowed edge is prevented as, again, it would require formation of a *meridional* product. The other edge is free for water entry and this pathway leads to the trans product.

The predictions of the AOM stereochemical model combined with the ligand constraints imposed by the neopentyl cap and the blocking by ligand arms are therefore in complete agreement with our observations and represent another success for the theory. Since the theory is based on an assumption of exclusive quartet-state reaction, this provides another piece of circumstantial evidence for our proposal that reaction in this complex occurs exclusively via the quartet state.

In summary, we conclude that $Cr(sen)^{3+}$ photoaquates to a single main product, *trans*-$Cr(sen\text{-}NH)(H_2O)^{4+}$. The doublet state has an abnormally short room temperature solution lifetime as a result of a radiationless process that competes with other processes depleting the doublet state. However, this doublet-state deactivation process does not lead to photoaquation but competes with BISC and photoaquation via the quartet state, resulting in an unprecedented reduction in photoaquation quantum yield on direct irradiation into the doublet state.

The photoinert nature of $Cr([18]\text{-}aneN_6)^{3+}$ probably arises because any labilized nitrogen atom is prevented, by its attachments to two neighbor coordination sites, from migrating to a new position as required in the AOM model. This would favor rapid recoordination accompanied by relaxation back to the ground state of the starting molecule.

IC010236J